Frascati Physics Series Vol. LVI (2012)
Dark Forces at Accelerators
October 16-19, 2012

Light Dark Gauge Boson Searches in Electroweak Processes

T. Beranek
Institut für Kernphysik and PRISMA Cluster of Excellence
Johannes Gutenberg-Universität Mainz, D-55099 Mainz

Abstract

Extending the Standard Model of particle physics by an $U(1)$ group generates an additional gauge boson γ' which is known as hidden or dark photon. The hidden photon is able to interact with the electromagnetic current of the Standard Model. We study the exploration reach of various fixed target experiments searching for the hidden photon. Therefore we investigate the creation of a lepton pair induced by quasi-elastic scattering of an electron beam off a heavy nucleus (A,Z), i.e. $e(A,Z) \to e(A,Z)e^+e^-$ with a hidden photon γ' as signal and a virtual photon as background in the intermediate state. We compare our calculations with the data taken in the test run of the MAMI experiment. Predictions of the expected exclusion limits of the 2012 beam time at MAMI are presented. Furthermore, our analysis of rare kaon decays as possibility to constrain the γ' parameter space is presented.

1 Introduction

Recent observations of anomalies in astrophysical data [1] have motivated to consider extensions of the Standard Model of particle physics (SM) by including an additional $U(1)$ gauge group which could explain such anomalies [2]. Though the idea to extend the SM by an additional $U(1)$ recently became popular, it did not rise up with these observations. In many well motivated SM extensions, e.g. from string theory, additional $U(1)$ groups appear naturally [3].
Extending the SM by such an $U(1)_D$ group generates an additional gauge boson γ' which is able to interact with the electromagnetic current of the Standard Model. Although this interaction is forbidden at tree level it is possible via kinetic mixing giving rise to an effective interaction Lagrangian

$$\mathcal{L}_{\text{int}} = i\,\varepsilon e\,\bar{\psi}_{\text{SM}}\,\gamma^{\mu}\,\psi_{\text{SM}}\,A'_{\mu},$$

where A' denotes the γ' field. Furthermore, ε is the kinetic mixing factor parameterizing the coupling strength relative to the electric charge e, and describes the interaction of the additional gauge boson with the electromagnetic current. The γ' may gain a mass $m_{\gamma'}$ which can be estimated to be in the range of 10 MeV to a few GeV, and the kinetic mixing factor $\varepsilon^2 = \alpha'/\alpha$ is predicted from various models to be in the range $10^{-12} < \varepsilon < 10^{-2}$ [4]. The coupling of the γ' to SM particles and the predicted mass range allows for the γ' search by accelerator experiments at modest energies with high intensities. The proposal to search for the hidden gauge boson by fixed-target experiments [5, 6] motivated several experimental programs, e.g. by the A1 Collaboration at the MAMI accelerator in Mainz [7] as well as at the CEBAF facility at Jefferson Lab [8, 9]. The A1 [7] and APEX [8] experiments already have published first data. In these electron-hadron scattering experiments an electron beam is scattered off a nuclear fixed target, and a lepton-antilepton pair is created, which is detected. Using the measured invariant mass distribution, a bump search is performed. In the case, that no bump is seen, an exclusion limit for the γ' coupling ε^2 as function of its mass $m_{\gamma'}$ can be calculated, for which a precise knowledge of the background is crucial. Such precise study is the main subject of the first part of the present work [10]. In the second part the possibility to constrain the γ' parameters from rare kaon decays is discussed [11].

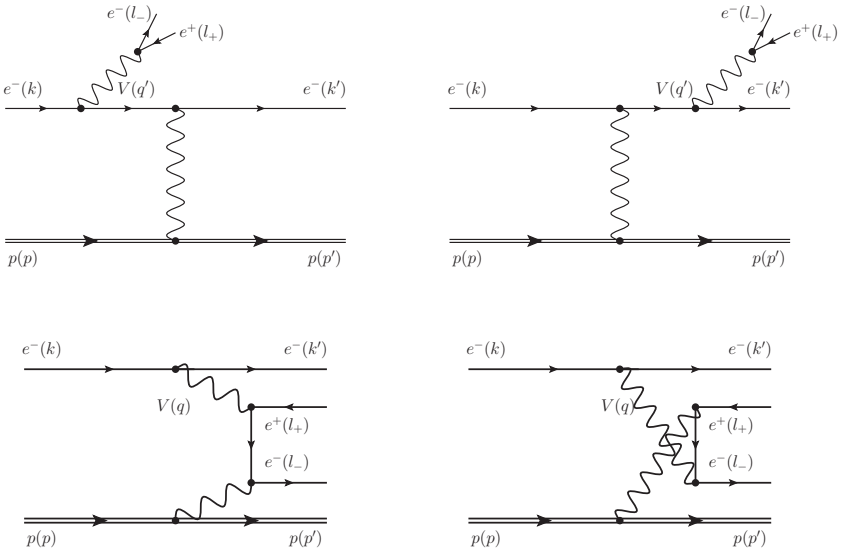

Figure 1: *Tree level Feynman diagrams contributing to the* $ep \to epl^+l^-$ *amplitude. Upper panel: exchange of the timelike boson* V *and a spacelike* γ *(TL). Lower panel: the spacelike boson* V *and a spacelike* γ *(SL). In addition to these direct (D) diagrams the exchange term (X), which consists of the same set of diagrams with scattered electron and electron of the* e^+e^- *pair exchanged, also contributes.*

2 Fixed target experiments

2.1 Calculation of the signal and background cross sections

The underlying diagrams for all fixed target experiments mentioned so far are shown in Fig. 1. We calculate this process exactly in leading order of QED and furthermore apply leading order radiative corrections of the corresponding elastic scattering process to obtain an estimate of these corrections, which reduce the cross section by an amount in the range of $10 - 20\,\%$.
The invariant amplitudes required for calculating the cross section can be read off from these Feynman diagrams. As in the two diagrams on the upper panel of Fig. 1 the intermediate boson V is timelike, we refer to this amplitude as TL. Correspondingly, we refer to the diagrams on the lower panel, where the

V is spacelike, as SL and their sum is denoted by SL + TL.
The isolated γ' production process is given by the coherent sum of the two TL diagrams on the upper panel of Fig. 1 while the background, resulting from the exchange of a virtual photon, is given by the sum over all diagrams, where the intermediate vector particle V in the TL diagrams is γ' and γ^*, respectively.
We assign a finite decay width $\Gamma_{\gamma'}$ to the γ'.

In the case that the l^+l^- pair and the beam lepton are of the same species, as for the existing experiments, the same diagrams of Fig. 1 with the scattered (beam) electron and created electron of the pair exchanged also have to be taken into account. Therefore, we refer to the diagrams depicted in Fig. 1 as "direct" contribution and to those with exchanged final state electrons as "exchange" contribution, labeled by D and X, respectively.
The nucleus spin as well as contributions from the breakup channel and nuclear excitations can be neglected to good approximation. Effects due to the nucleus spin are suppressed by the large nucleus mass, which can be checked analytically. The inelastic contribution can be neglected since the momenta transferred to the nucleus are small.

The comparison with experimental data can be performed by integrating the obtained differential cross section over the experimental acceptances. To obtain the acceptance integrated cross section $\Delta\sigma$, which can be related to experimental count rates by multiplication with the luminosity, a non-trivial 8-fold integration is necessary.
The signal cross section $\Delta\sigma_{\gamma'}$ can be related to the direct TL cross section $\Delta\sigma_\gamma^{\mathrm{TL}}$ as given in Eq. (19) by Bjorken et. al. [5]

$$\frac{\Delta\sigma_{\gamma'}}{\Delta\sigma_\gamma^{\mathrm{TL}}} = \frac{3\pi}{2N}\frac{\varepsilon^2}{\alpha}\frac{m_{\gamma'}}{\delta m}. \tag{1}$$

Using this quantity one can calculate a limit on ε as

$$\varepsilon^2 = \left(\frac{\Delta\sigma_{\gamma'+\gamma}}{\Delta\sigma_\gamma} - 1\right)\frac{\Delta\sigma_\gamma}{\Delta\sigma_\gamma^{\mathrm{TL}}}\frac{2\,N\,\alpha}{3\pi}\frac{\delta m}{m_{\gamma'}}, \tag{2}$$

where the ratio $\Delta\sigma_{\gamma'+\gamma}/\Delta\sigma_\gamma$ is the (aimed) signal sensitivity, which has to be determined from the experiment. The ratio of the background cross section to the direct TL cross section $\Delta\sigma_\gamma/\Delta\sigma_\gamma^{\mathrm{TL}}$ has to be determined from theory.

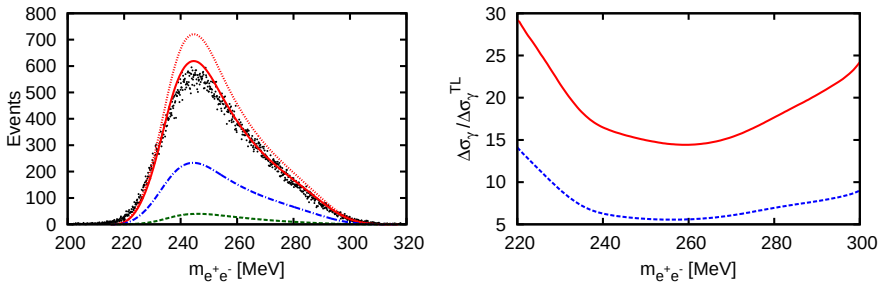

Figure 2: *Left panel: Comparison of theory calculations and experimental data for a $m_{e^+e^-}$ bin width of* 0.125 MeV. *Black points: Data taken in a particular run of the MAMI 2010 experiment* [7]. *Solid curve: Theory calculation of the background cross section. Dotted curve: Theory calculation of the background cross section without radiative corrections. Dashed-dotted curve: Theory calculation of the direct SL + TL cross section. Dashed curve: Theory calculation of the direct TL cross section. Right panel: Solid (dashed) curve: Ratio of the background cross section $\Delta\sigma_{\gamma,\,\mathrm{D+X}}$ ($\Delta\sigma_{\gamma,\,\mathrm{D}}$) to the direct TL cross section $\Delta\sigma_\gamma^{TL}$, respectively.*

2.2 Comparison with data and predictions for MAMI

A first test run to proof the feasibility of a dedicated γ' fixed target search experiment has been performed at MAMI by the A1 Collaboration in 2010 [7]. A sample of the data taken in this experiment compared to our calculations can be seen in Fig.2.
For the comparison of the calculation and the data integrated luminosity of $\mathcal{L} = 41.4\,\mathrm{fb}^{-1}$ for the selected sample of events is used. A background contribution of around 5% was already subtracted in this sample, the systematic uncertainty in the luminosity from the knowledge of the thickness of the target foil is below 5%.

As seen on the left panel of Fig. 2, our calculation (solid curve) of the radiative background and the experimental data (points) are in good agreement. The influence of the radiative corrections is displayed by the solid and dotted curve on Fig. 2 which are calculated with and without radiative corrections, respectively.

One notices from the right panel of Fig. 2 (solid curve) that the ratio $\Delta\sigma_{\gamma,\,\mathrm{D+X}}/\Delta\sigma_\gamma^{\mathrm{TL}}$ smoothly varies between 15 and 25 for most of the invariant

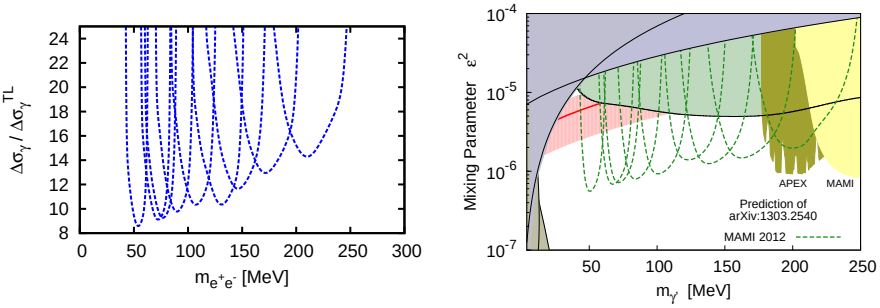

Figure 3: *Left panel: Combined plot of our result for the ratios* $\Delta\sigma_\gamma/\Delta\sigma_\gamma^{TL}$ *of each setting probed in the MAMI 2012 experiment, starting with the lowest beam energy on the left. Right panel: Predicted exclusion limits for the MAMI 2012 experiment.*

mass range. Neglecting the necessary contribution of the exchange term to the cross section, the ratio is lower by a factor of about 3 for the investigated range (dashed curve on the right panel of Fig. 2). The A1 Collaboration started a γ' search run at MAMI in 2012, probing the kinematics centered around $m_{e^+e^-} = 57 - 218\,\mathrm{MeV}$, in which no signal of a γ' was found. In Fig. 3 a combined plot of our result for the ratio $\Delta\sigma_\gamma/\Delta\sigma_\gamma^{\mathrm{TL}}$ is shown for each setting as function of the invariant mass $m_{e^+e^-}$. One obtains for the ratio a value of around $10 - 15$.

On the right panel of Fig. 3, the exclusion limits on ε^2 [5, 7, 8, 12] are displayed: the shaded regions show existing limits, whereas the dashed curves show our predictions for the MAMI set of kinematics indicated by the dashed curve for an assumed integrated luminosity of around $10\,\mathrm{fb}^{-1}$. Obviously, the MAMI 2012 will cover a large part of the $(g-2)$ welcome band.

3 Rare Kaon decays

In the following we will study the process $K^+ \to \mu^+\nu_\mu\gamma'$ as a possible signal from the dark sector (see Feynman diagram in Fig. 4) within the mentioned framework of kinetic mixing (model I) as well as in a model where the γ' couples only to the muon assuming an explicit breaking of gauge invariance [13] (model II). In a pioneering experiment [14] of the decay $K^+ \to \mu^+ +$ neutrals, only the

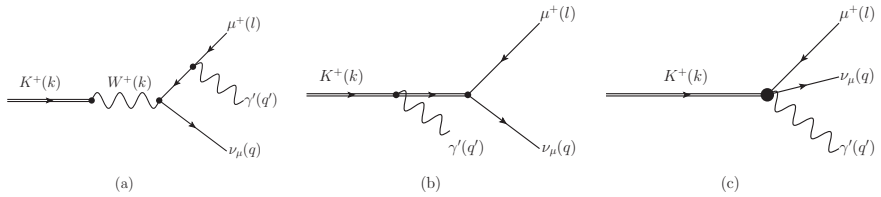

Figure 4: *Feynman diagram for the process* $K^+ \to \mu^+\nu_\mu\gamma'$.

charged muon is detected, excluding further charged particles or photons in the final state. Therefore it is convenient to express the decay rates as functions of the kinetic energy of the muon T_μ. In this experiment an upper bound for the branching fraction $\Gamma(K^+ \to \mu^+ + \text{ neutrals})/\Gamma(K^+ \to \mu^+\nu)$ of $2 \cdot 10^{-6}$ was found.

The SM background for invisible γ' decays results from the $K^+ \to \mu^+\nu_\mu\nu_l\bar{\nu}_l$ decays. Due to the applied experimental cuts a further background arising from radiative corrections to the 2-body decay $K \to \mu\nu_\mu$ can be neglected.

In order to obtain a dimensionless quantity, it is helpful to consider the ratio of these decay rates relative to the ratio of the 2-body decay $K^+ \to \mu^+\nu_\mu$. In order to obtain the experimental limits from these data the differential decay rate $\frac{d\Gamma}{dE_\mu}(K^+ \to \mu^+\nu_\mu\gamma')$ has to be folded with the detector efficiency $D(E_\mu)$ [14], i.e.

$$\tilde{R}(m_{\gamma'}) := \frac{\int \frac{d\Gamma}{dE_\mu}(K^+ \to \mu^+\nu_\mu\gamma')D(E_\mu)dE_\mu}{\Gamma(K^+ \to \mu^+\nu_\mu)}. \tag{3}$$

Since the kinetic mixing factor ε is a global factor of the amplitudes obtained from Fig. 4, one can rewrite $\tilde{R}\ (m_{\gamma'}) = \varepsilon^2\ R\ (m_{\gamma'})$ and thus finds an upper bound for the allowed values of ε^2 as:

$$\varepsilon^2 < \frac{2 \cdot 10^{-6}}{R(m_{\gamma'})}. \tag{4}$$

In Fig. 5 (upper and middle panels) the differential decay rate for the signal process relative to the decay $K^+ \to \mu^+\nu_\mu$ is shown calculated within model I and II for the full phase space (left panels) and with applied corrections due to the given detector acceptance (right panels), according to the experimental set-up [14]. One notices that within the kinetic mixing model (upper panels of Fig. 5) the inner bremsstrahlung contribution (IB) completely dominates the

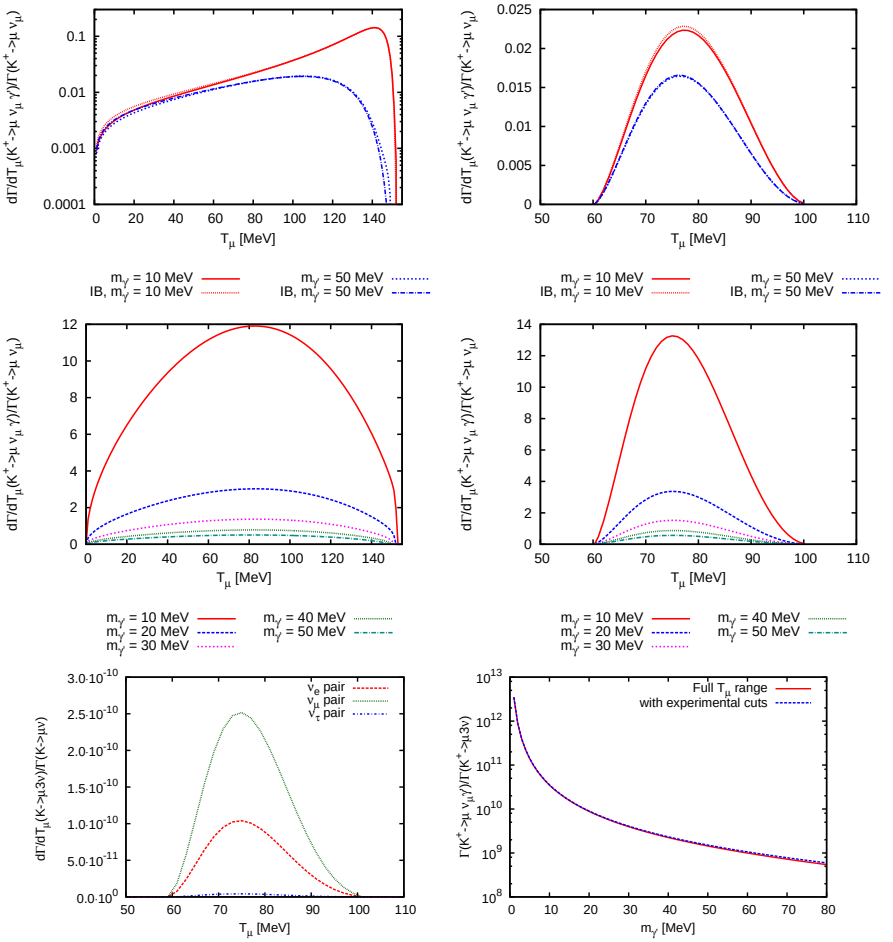

Figure 5: *Upper and middle panels: Ratio of* $\frac{d\Gamma}{dT_\mu}(K^+ \to \mu^+\nu_\mu\gamma')$ *and* $\Gamma(K^+ \to \mu^+\nu_\mu)$ *for various* γ' *masses for perfect detector efficiency (left panels) and for finite detector efficiency* [14] *(right panels) at* $\varepsilon^2 = 1$. *Upper panels: kinetic mixing model (model I); middle panels: model II, where the* γ' *only couples to the* μ^+. *Lower left panel: Standard Model background for different neutrino families using the detector efficiency function. Lower right panel: ratio of total decay rates* $\Gamma(K^+ \to \mu^+\nu_\mu\gamma')$ *at* $\varepsilon^2 = 1$ *relative to* $\Gamma(K^+ \to \mu^+\nu_\mu\nu\bar{\nu})$ *in model II.*

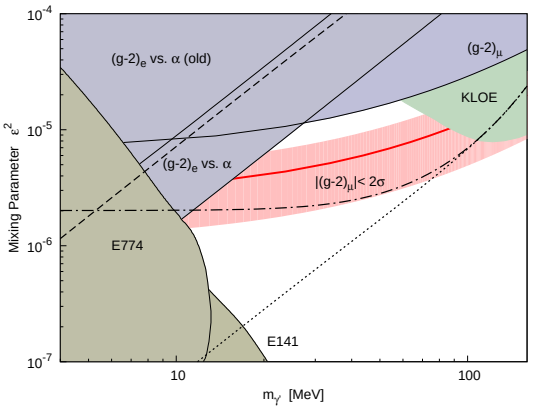

Figure 6: *Exclusion limits on the γ' parameter space (see text for further details). Dashed-dotted curve: bound calculated in the kinetic mixing model (model I) for an accuracy of the ratio $\Gamma(K^+ \to \mu^+\nu_\mu\gamma')/\Gamma(K^+ \to \mu^+\nu_\mu)$ of 10^{-9}. Dashed curve: result for the 1973 data [14] within model II, where the γ' only couples to the μ^+. Dotted curve: bound calculated in model II for an assumed improvement of the experimental accuracy by two orders of magnitude, i.e. $2 \cdot 10^{-8}$.*

result for the considered γ' mass parameters: comparison between IB curves and curves including the form factor dependence [15, 16]. Since in model II the gauge invariance is not required, the decay rate is enhanced by a factor of $1/m^2_{\gamma'}$ compared to model I. The expected SM background from the decay $K^+ \to \mu^+\nu_\mu\nu\bar{\nu}$ with the applied experimental cuts [14] is shown on the lower left panel.

As one can see from the lower right panel of Fig. 5, the total γ' decay rate (model II) $\Gamma(K^+ \to \mu\nu_\mu\gamma')$ calculated with $\varepsilon^2 = 1$ is about a factor of 10^9 larger than the decay rate to SM particles $\Gamma(K^+ \to \mu^+\nu_\mu\nu_l\bar{\nu}_l)$. This corresponds to an γ' signal, which will dominate over the expected SM signal for mixing factors down to $\varepsilon^2 \simeq 10^{-9}$. The calculated limits on the γ' parameter space are shown in Fig. 6. In this figure the colored regions again correspond to already excluded configurations of mass and coupling strength [17]. In this plot we have included the old as well as the new exclusion limits from $(g-2)$ of the electron compared to the fine structure constant α. One has to dis-

tinguish limits from searches with visible and invisible decay products. The exclusion limits in Fig. 6 are all obtained within the kinetic mixing framework were the γ' decay is assumed to be into SM leptons, except those from rare kaon decays in model I. In this work the bounds obtained from the kinetic mixing model (model I) correspond to searches with visible decay products. In experiments therefore the process $K^+ \to \mu^+\nu_\mu e^+e^-$, would be investigated e.g. by a search for peaks appearing over the known SM background. For invariant masses of the e^+e^- $m_{ee} < 2m_\mu$ the branching ratios $\Gamma(K^+ \to \mu^+\nu_\mu\gamma')$ and $\Gamma(K^+ \to \mu^+\nu_\mu e^+e^-)(m_{ee} = m_{\gamma'})$ after full phase space integration are equal. In model II the kaon decay to γ' is assumed to be invisible. Therefore the existing limits from direct searches in Fig. 6 do not exactly apply here. For reasons of simplicity we use the same figure to illustrate the numerical results of this calculation.
A possible bound for the kinetic mixing model is represented by the dash-dotted curve for an assumed experimental accuracy of the ratio $\Gamma(K^+ \to \mu^+\nu_\mu\gamma')/\Gamma(K^+ \to \mu^+\nu_\mu)$ of 10^{-9}. Furthermore, in Fig. 6 the bound obtained in model II and an estimate in which way the exclusion limits change due to an improvement in the experimental accuracy of the ratio $\Gamma(K^+ \to \mu^+\nu_\mu\gamma')/\Gamma(K^+ \to \mu^+\nu_\mu)$ by two orders of magnitude (dotted curve) are shown. Such an improved extraction might be achieved by new facilities, such as the NA62 experiment at CERN or rare kaon decay experiments at JPARC.

4 Conclusions

We have calculated the cross sections for the γ' fixed target experiments $e(A,Z) \to e(A,Z)l^+l^-$. We find, that our calculations for the electromagnetic background processes are in good agreement with the data taken at MAMI. This allows us to give accurate predictions for future exclusion limits as presented here for the new MAMI experiment, and we find, that the largest part of the $(g-2)_\mu$ welcome can be excluded.
Furthermore, we have investigated rare kaon decays as possibility to explore the γ' parameter space in the low mass region. We have shown, that the method used in this work may be suited to extend the existing limits within two models for the γ' coupling. For that purpose more precise data are necessary.

5 Acknowledgements

This work was done in collaboration with H. Merkel and M. Vanderhaeghen. This work was supported in part by the Research Centre "Elementarkräfte und Mathematische Grundlagen" at the Johannes Gutenberg University Mainz, the federal state of Rhineland-Palatinate, and in part by the Deutsche Forschungsgemeinschaft DFG through the Collaborative Research Center "The Low-Energy Frontier of the Standard Model" (SFB 1044), and the Cluster of Excellence "Precision Physics, Fundamental Interactions and Structure of Matter" (PRISMA). TB likes to thank Björn Walk for helpful discussions on GPU programming. Furthermore, we thank Achim Denig for useful discussions.

6 References

References

1. A. W. Strong *et al.*, Astron. Astrophys. **444**, 495 (2005). O. Adriani *et al.* [PAMELA Collaboration], Nature **458**, 607 (2009). I. Cholis, G. Dobler, D. P. Finkbeiner, L. Goodenough and N. Weiner, Phys. Rev. D **80**, 123518 (2009).

2. N. Arkani-Hamed, D. P. Finkbeiner, T. R. Slatyer and N. Weiner, Phys. Rev. D **79**, 015014 (2009). M. Pospelov and A. Ritz, Phys. Lett. B **671**, 391 (2009).

3. S. Weinberg, Phys. Rev. Lett. **40**, 223 (1978). L. B. Okun, Sov. Phys. JETP **56**, 502 (1982). B. Holdom, Phys. Lett. B **178**, 65 (1986). P. Fayet, Nucl. Phys. B **347**, 743 (1990). M. Pospelov, Phys. Rev. D **80**, 095002 (2009). S. Andreas, M. D. Goodsell and A. Ringwald, Phys. Rev. D **87**, 025007 (2013).

4. P. Fayet, Phys. Rev. D **75**, 115017 (2007). C. Cheung, J. T. Ruderman, L. -T. Wang and I. Yavin, Phys. Rev. D **80**, 035008 (2009). R. Essig, P. Schuster and N. Toro, Phys. Rev. D **80**, 015003 (2009). M. Goodsell, J. Jaeckel, J. Redondo and A. Ringwald, JHEP **0911**, 027 (2009).

5. J. D. Bjorken, R. Essig, P. Schuster and N. Toro, Phys. Rev. D **80**, 075018 (2009).

6. B. Batell, M. Pospelov and A. Ritz, Phys. Rev. D **79**, 115008 (2009). M. Reece and L. -T. Wang, JHEP **0907**, 051 (2009). B. Batell, M. Pospelov and A. Ritz, Phys. Rev. D **80**, 095024 (2009).

7. H. Merkel *et al.* [A1 Collaboration], Phys. Rev. Lett. **106**, 251802 (2011).

8. R. Essig, P. Schuster, N. Toro and B. Wojtsekhowski, JHEP **1102**, 009 (2011). S. Abrahamyan *et al.* [APEX Collaboration], Phys. Rev. Lett. **107**, 191804 (2011).

9. The Heavy Photon Search Collaboration (HPS), `https://confluence.slac.stanford.edu/display/hpsg/`. M. Freytsis, G. Ovanesyan and J. Thaler, JHEP **1001**, 111 (2010). Y. Kahn and J. Thaler, Phys. Rev. D **86**, 115012 (2012).

10. T. Beranek, H. Merkel and M. Vanderhaeghen, arXiv:1303.2540 [hep-ph].

11. T. Beranek and M. Vanderhaeghen, Phys. Rev. D **87**, 015024 (2013).

12. S. Andreas, C. Niebuhr and A. Ringwald, Phys. Rev. D **86**, 095019 (2012). D. Babusci *et al.* [KLOE-2 Collaboration], arXiv:1210.3927 [hep-ex].

13. B. Batell, D. McKeen and M. Pospelov, Phys. Rev. Lett. **107**, 011803 (2011).

14. C. Y. Pang *et al.*, Phys. Rev. D **8**, 1989 (1973).

15. J. Bijnens, G. Ecker and J. Gasser, Nucl. Phys. B **396**, 81 (1993).

16. A. A. Poblaguev *et al.*, Phys. Rev. Lett. **89**, 061803 (2002).

17. F. Archilli *et al.*, Phys. Lett. B **706**, 251 (2012). H. Davoudiasl, H. -S. Lee and W. J. Marciano, Phys. Rev. D **86**, 095009 (2012).